










# Time-Dependent Errors Influence on the Transmission Error in Planetary Gears with Different Mesh Phasing

J. Sanchez-Espiga<sup>1,2</sup> , M. Fürst<sup>2</sup> , A. Fernandez-del-Rincon<sup>1</sup> , M. Otto<sup>2</sup> ,  
F. Viadero<sup>1</sup>  , and K. Stahl<sup>2</sup> 

<sup>1</sup> Universidad de Cantabria, 39005 Santander, Cantabria, Spain  
viaderof@unican.es

<sup>2</sup> TUM School of Engineering and Design, Institute of Machine Elements, Gear Research Center (FZG), Technical University of Munich (TUM), Garching, Germany

**Abstract.** This work focuses on the effect of time-dependent errors in the behavior of planetary transmissions. More precisely, this work analyses the response of low-speed planetary transmissions to the presence of time-varying manufacturing errors such as run-out and index errors, which are some of the most common errors inherent to the gear manufacturing process. Thus, in order to observe the interaction of these transmissions to the presence of those errors the analysis focuses on its transmission error. In the context of this work transmissions with in-phase and sequentially phased mesh phasing are considered. These transmissions also implement a pair of state-of-the-art roller bearings modelled in the sun support. As a result of the error modelling, it is possible to see how the results for in-phase transmissions are not affected by the size of the error. However, in the sequentially phased transmissions the change in the geometry of the contacts varies the mesh phasing and leads to discrepancies in the transmission's behavior.

**Keywords:** Planetary transmissions · Spur gears · Roller bearings · Transmission error

## 1 Introduction

In today's society, gear transmissions are a commonly used solution to transmit power in a number of different applications. In the field of gear transmissions many different configurations are available and one common configuration is planetary gear transmissions. These transmissions are experiencing an ongoing growth in their applicability, from more classical applications such as internal combustion vehicles [1], to more recent applications as electrical vehicles [2], wind generators [3, 4], and aircrafts [5, 6].

The raise in the interest on gear transmission analysis is patent in the increment on the number of publications related to this field [7]. This growth led to the development of new models to analyze the behavior of these transmissions at a lower cost than experimental studies. However, these models provide several different solutions that present a variety

of advantages and disadvantages depending on the chosen formulation. Thus, analytical models provide a great ratio between accuracy and computational effort, but the degree of detail that can be included is limited. On the other hand, it is possible to opt for a more advanced formulation by defining a finite element model of the transmission. This raises the degree of accuracy in the results, however, raises the computation time. Therefore, from the advantages of both these approaches the proposal to combine them [8] and extract the main advantages from each, avoiding the majority of the inconveniences, resulted in the development of a wide range of hybrid models [9–11].

These models are employed to analyze the static and dynamic performance of planetary transmissions. One of the common applications of these models is the simulations of the transmission's performance under the presence of several inherent manufacturing errors [12–16]. However, these studies focus normally on the impact of manufacturing errors such as pinhole-position and tooth thickness errors that do not vary in time. On the other hand, various different studies observe the impact of time-dependent errors in the planetary transmission's load sharing [12, 15, 17].

This work sets the focus on the behaviour of planetary transmissions affected by time-dependent errors (run-out and index errors), however, in the dynamics of this transmission for low-speed performance given their importance in some industrial applications and its relation to the NVH. In addition, the transmission's behaviour includes the effect of a pair of roller bearings in the sun support. This study is performed for a number of scenarios that contemplate in-phase and sequentially phased transmissions, as well as several different error sizes both for eccentricity and index errors.

## 2 Methods

This section gathers all the relevant details of the algorithms employed to recreate the transmissions that are the object of study in this work. Thus, at the beginning the specifics regarding the hybrid model employed for the simulations are given. Then, the implementation of the roller bearings is presented. Finally, the modelling of the time-dependent errors is included.

### 2.1 Hybrid Model

The model employed in this work [10] consists of an analytical-finite-element hybrid model that is based on the proposal presented by Vedmar and Henriksson in [18]. Therefore, this model is developed in two different lines. The first of them, the use of analytical formulations to solve the geometrical problem regarding the contact between external and internal gears with involute profile teeth. Thus, to this aim this model considers the possible contacts between a  $Z$  number of teeth.

$$Z = 2 \cdot \text{ceil}(\varepsilon + 1) \quad (1)$$

Then, with this formulation for a common contact ratio ( $\varepsilon$ ), which for spur gears is between 1 and 2, the number of possible contacts that are considered is 6. However, this formulation provides the opportunity to study also high-contact ratio spur gears, where the contact ratio is over 2.

Afterwards, the algorithms employed to determine the distance between flanks of opposite gears are employed, these formulae are covered in detail in [10]. As a singularity of this proposal both gears and their teeth are considered infinitely solid rigids and they are allowed to overlap with one another. Consequently, the indicative of an existing contact is the existence of a positive overlap.

On the other hand, while the overlaps are determined the contact solving algorithm is activated. This algorithm is the part of the model where the hybrid approach is necessary and determinant. On the one hand, a pair of finite element models, as seen in [10, 18, 19], are defined for each kind of gear that composes the planetary transmission. Thus, these models are used to solve the linear part of the contact problem, which consists in determining the deformations in the teeth and body of the gear due to the application of the contact force somewhere along the tooth profile. To this aim, these finite element models are a global one, which represents the body of the gear and the same  $Z$  number of teeth calculated in (1). The other finite element model consists in a local model that represents the profile of the active flank to a depth  $h$ . By employing the superposition principle, as seen in [10, 18, 20], it is possible to eliminate the distortion related to the application of a point load in the finite element models and obtain the deflections both in the teeth and body of the gear.

While the linear part of the contact is solved, the analytical formulation presented by Weber and Banaschek in [21] and modified by Iglesias et al. for internal gears in [10] is employed to iteratively converge to a solution for the local contact.

Once this procedure is finished and all the pieces are put together, the contact forces in all the existing contacts are known, as well as the effects of the flexibility of the elements.

Thus, with the results to the contact forces, the next step is determining if there is balance in the transmission. In this current case, balance refers to the balance in the power transmission between the input and output elements, considering there are no losses due to any effect, the torque balance in each planet, considering its simultaneous contact with the sun and ring gears. Finally, the balance in the sun gear support between the contacts and the support force, as shown in [14].

## 2.2 Non-linear Roller Bearings

As far as the bearings are concerned, the data employed for its modelling correspond to the characteristics of a NU1008-XL-M1 manufactured by Schaeffler. This bearing is modelled in LAGER2 [22, 23]. As a result, the values of the deflections suffered by the original configuration of the bearing can be calculated for given loads. This allows its implementation in the hybrid model presented above. This consists in the use of numerical splines to convert the discretized values provided by LAGER2 into a continuous function within the scope of loads considered, as seen in Fig. 1.

For every iteration of the non-linear contact problem solver, the balance problem in the transmission is analyzed. Beyond reaching the balance or not, the algorithm calculates a force in the support of the sun gear. These positions are taken from the initial conditions provided for the calculation. Thus, with the deflection, the force in the bearing is established.

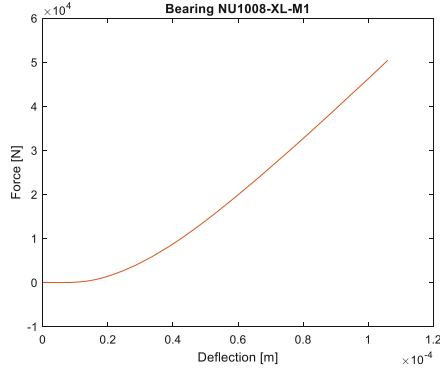


**Fig. 1.** Diagram of the force-deflection ratio in the NU1008-XL-M1 roller bearing.

The non-linearities in the behavior of the bearing increases the degree of realism reached in the simulation, but at the cost of a higher computation time.

### 2.3 Time-Dependent Errors Definition

The hybrid model employed for this work provides the opportunity of including several different manufacturing and mounting errors. Thus, in this case, the focus is set on time-dependent errors, and among the gamut of possibilities the ones chosen are the eccentricity error and index errors. Both these errors are implemented in the sun gear, where the bearings are mounted, too.

Starting off with the eccentricity error, it depends completely on the angular position of the gear where it exists. Therefore, it is modeled by defining the maximum magnitude of this error and applying the sinusoidal function necessary to recreate the influence of the shaft rotation in the error, as the following:

$$e_{ecc}(\theta_S) = A_{ecc} \cdot \cos(\theta_S + \varphi) \quad (2)$$

Thus,  $A_{ecc}$  is the amplitude of the sinusoidal wave that defines the time dependent eccentricity error,  $\theta_S$  is the actual rotation in the sun gear, and  $\varphi$  is the phasing.

As far as the index error is concerned, it can be modelled in many different ways. The actual index error consists in an advancement or delay between the actual position of a tooth in a gear and the ideal position of that tooth. However, in this case, considering the gear cutting process, it is modelled as a function dependent on the sun gear rotation, as presented in [24].

$$e_{ind}(\theta_S) = \sum_{n=1}^N A_n \cdot \sin\left(n \cdot \text{floor}\left(\frac{\theta_S}{\theta_{pS}}\right) \cdot \theta_{pS}\right) \quad (3)$$

where  $A_n$  is the error amplitude in the  $n$ th harmonic, the  $\theta_S$  is the actual rotation in the sun gear,  $\theta_{pS}$  is the pitch angle in the sun, and the floor function rounds double number to the closest lower or equal integer number.

### 3 Working Configurations

This study focuses on the behavior of low speed 3-planet planetary gears whose geometrical specifications are gathered in Table 1.

**Table 1.** Specifics of the tooth profile

Characteristic	Magnitude
Module (mm)	4
Pressure angle (°)	20
Addendum (mm)	1 m
Dedendum (mm)	1.25 m
Tip rounding arc radius (mm)	0.05 m

The number of teeth defined for each gear is gathered in the Table 2. Thus, a pair of transmissions are considered. In the first, every sun-planet or planet-ring contact happen at the same time, therefore, the mesh phasing is in-phase. This transmission is Equally Spaced In-Phase (ESIP). Then, the second configuration considered includes a delay in the mentioned contacts, therefore, it is Equally Spaced Sequentially Phased (ESSP) as seen in [14].

**Table 2.** Number of teeth in each gear for the studied configurations

Configuration	$Z_S$	$Z_P$	$Z_R$
ESIP	30	29	90
ESSP	29	30	91

In addition, this study considers two different errors. These errors, defined in Sect. 2.3, are eccentricity and index errors and their amplitudes are given in Table 3.

**Table 3.** Eccentricity and index errors amplitudes

Error	Amplitude ( $\mu\text{m}$ )		
Eccentricity	10	30	50
Index	10	30	50

Finally, these simulations are performed for an input torque of 2000 Nm. In addition, in order to observe the effect of these periodic errors and extract the most relevant information of the results the simulations are carried out up to 15 meshing cycles in the sun of input element rotation.

## 4 Results

In this section the results obtained for the simulations established previously in this work are gathered. At first, the focus is set on the transmission error in these planetary transmissions under the presence of the mentioned errors. Then, the sun gear orbits in those same scenarios are extracted and analyzed.

### 4.1 Transmission Errors

First of all, this work focuses on low-speed transmissions, therefore, the dynamic effects have not been considered in the transmission error (TE).

On these grounds, in Fig. 2 the results obtained for the ESIP transmission with a  $10\ \mu\text{m}$  eccentricity and index errors are presented. It is possible to see how even though the definition of the errors is similar, but not identical, the results obtained for the TE are almost identical. In order to extend the analysis, the same results are presented for the ESIP transmission, but in this case with  $50\ \mu\text{m}$  eccentricity and index errors. As seen in Fig. 3 the results are identical to the previous ones.

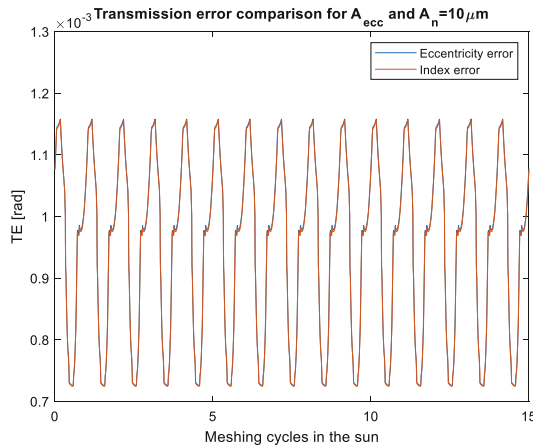


**Fig. 2.** Transmission error comparison for ESIP transmissions with a  $10\ \mu\text{m}$  error

This leads to think that the interaction between the gear and the roller bearings are making that the rotational behavior of the sun gear is the same for any of the scenarios considered.

The next step is to analyze these scenarios, but for the ESSP transmission, in which a priori a change in the geometry of contacts can be expected to have a more significant effect in the TE results. At first, in Fig. 4 the case with  $30\ \mu\text{m}$  eccentricity and index errors are presented and compared.

It is possible to see how the influence of the error in ESSP transmissions is visible, first of all, and both errors have a different behavior. In fact, seeing the results obtained for  $30\ \mu\text{m}$  (Fig. 4) and  $50\ \mu\text{m}$  (Fig. 5) eccentricity and index errors it is possible to

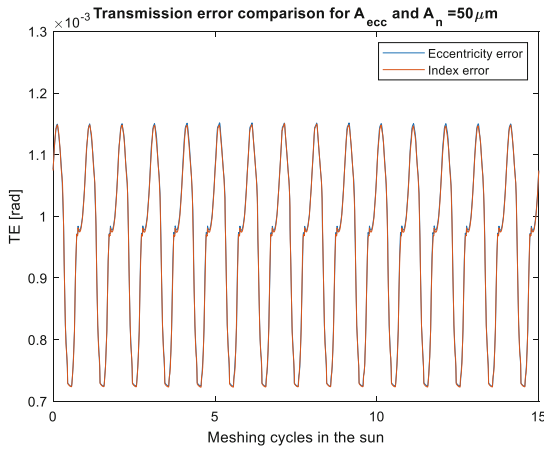


**Fig. 3.** Transmission error comparison for ESIP transmissions with a  $50 \mu\text{m}$  error.

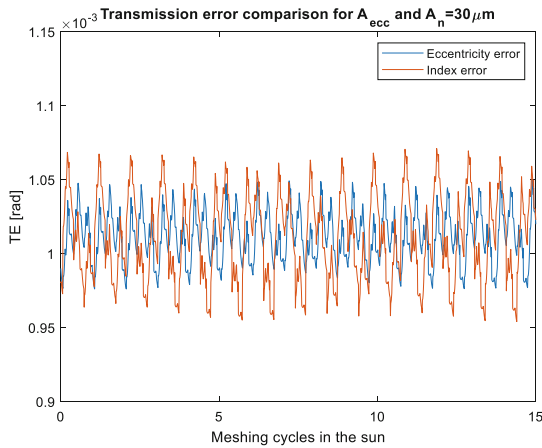


**Fig. 4.** Transmission error comparison for ESSP transmissions with a  $30 \mu\text{m}$  error.

observe how the TE in the sun in both under each error does not resemble any other scenario.

These changes are related to the variation in the mesh phasing due to the errors. Furthermore, the change in the mesh phasing is different for each kind of error and becomes more influential as the error grows. These errors have an impact also in the peak-to-peak value, however, the index error prove to be more impactful in the transmission's behavior as far as TE is concerned.

## 5 Conclusions

The conclusions that can be extracted to the current analysis are the following:

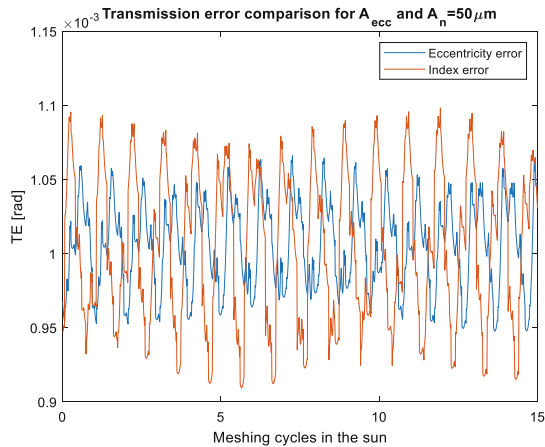


**Fig. 5.** Transmission error comparison for ESSP transmissions with a 50  $\mu\text{m}$  error.

- The transmission error in ESIP transmissions under the impact of an eccentricity or index sinusoidal error is identical and is not affected by the size of the error.
- The change in the mesh phasing due to the errors does modify the TE in the ESSP transmissions, whereas in the TE for ESIP transmissions the changes due to the implemented errors are not visible in the TE.
- The peak-to-peak value of the TE in ESIP transmissions does not vary with the error. However, in the ESSP transmissions it does vary, reaching higher values for the index error.

**Acknowledgements.** The authors from Universidad de Cantabria would like to thank the Spanish Ministry of Science and Innovation for financing the project PID2020-116213RB-I00, in which context Dr. J. Sanchez-Espiga completed a postdoctoral research stay at the Gear Research Center (FZG), Technical University of Munich (TUM), Garching, Germany.

## References

1. Inalpolat, M., Kahraman, A.: Dynamic modelling of planetary gears of automatic transmissions. *Proc. Inst. Mech. Eng. Part K J. Multi-body Dyn.* **222**(3), 229–242 (2008). <https://doi.org/10.1243/14644193JMBD138>
2. Du, W., Zhao, S., Jin, L., Gao, J., Zheng, Z.: Optimization design and performance comparison of different powertrains of electric vehicles. *Mech. Mach. Theory* **156**, 104143 (2021). <https://doi.org/10.1016/j.mechmachtheory.2020.104143>
3. Viadero, F., Fernández, A., Iglesias, M., De-Juan, A., Liaño, E., Serna, M.A.: Non-stationary dynamic analysis of a wind turbine power drivetrain: offshore considerations. *Appl. Acoust.* **77**, 204–211 (2014). <https://doi.org/10.1016/j.apacoust.2013.10.006>
4. Diez-Ibarbia, A., Sanchez-Espiga, J., Fernandez-del-Rincon, A., Calvo-Irisarri, J., Iglesias, M., Viadero, F.: Probabilistic analysis of the mesh load factor in wind-turbine planetary transmissions: tooth thickness errors. *Mech. Mach. Theory* **185**, 105341 (2023). <https://doi.org/10.1016/j.mechmachtheory.2023.105341>



5. Götz, J., Siglmüller, F., Fürst, M., Otto, M., Stahl, K.: Experimental investigation of the dynamic load sharing of planetary gearboxes. *Forsch. im Ingenieurwes.* (2021). <https://doi.org/10.1007/s10010-021-00507-5>
6. Kurzke, J.: Fundamental differences between conventional and geared turbopumps. *Proc. ASME Turbo Expo* **1**, 145–153 (2009). <https://doi.org/10.1115/GT2009-59745>
7. Cooley, C.G., Parker, R.G.: A review of planetary and epicyclic gear dynamics and vibrations research. *Appl. Mech. Rev.* **66**(4), 040804 (2014). <https://doi.org/10.1115/1.4027812>
8. Vijayakar, S.: A combined surface integral and finite element solution for a three-dimensional contact problem. *Int. J. Numer. Methods Eng.* **31**(3), 525–545 (1991). <https://doi.org/10.1002/nme.1620310308>
9. Abovsliman, V., Velez, P., Becquerelle, S.: Modeling of spur and helical gear planetary drives with flexible ring gears and planet carriers. *J. Mech. Des. Trans. ASME* **129**(1), 95–106 (2007). <https://doi.org/10.1115/1.2359468>
10. Iglesias, M., Fernandez del Rincon, A., de-Juan, A., Diez-Ibarbia, A., Garcia, P., Viadero, F.: Advanced model for the calculation of meshing forces in spur gear planetary transmissions. *Meccanica* **50**(7), 1869–1894 (2015). <https://doi.org/10.1007/s11012-015-0130-3>
11. Guilbert, B., Velez, P., Cutuli, P.: Quasi-static and dynamic analyses of thin-webbed high-speed gears: centrifugal effect influence. *Proc. Inst. Mech. Eng. Part C J. Mech. Eng. Sci.* **233**(21–22), 7282–7291 (2019). <https://doi.org/10.1177/0954406219855411>
12. Bodas, A., Kahraman, A.: Influence of carrier and gear manufacturing errors on the static load sharing behavior of planetary gear sets. *JSME Int. J. Ser. C* **47**(3), 908–915 (2004). <https://doi.org/10.1299/jsmec.47.908>
13. Iglesias, M., Fernandez del Rincon, A., De-Juan, A., Garcia, P., Diez-Ibarbia, A., Viadero, F.: Planetary transmission load sharing: manufacturing errors and system configuration study. *Mech. Mach. Theory* **111**, 21–38 (2017). <https://doi.org/10.1016/j.mechmachtheory.2016.12.010>
14. Sanchez-Espiga, J., Fernandez-del-Rincon, A., Iglesias, M., Viadero, F.: Influence of errors in planetary transmissions load sharing under different mesh phasing. *Mech. Mach. Theory* **153**, 104012 (2020). <https://doi.org/10.1016/j.mechmachtheory.2020.104012>
15. Kahraman, A.: Static load sharing characteristics of transmission planetary gear sets : model and experiment. In: *Transmission Driveline System Symposium*, no. 1, pp. 1–10 (1999). <https://doi.org/10.4271/1999-01-1050>
16. Huo, G., Sanchez Espiga, J., Iglesias, M., Fernandez del Rincon, A., Viadero, F., Jiao, Y.: Influence of manufacturing errors on the behaviour of a two-stage planetary gear train. In: *DYNA*, vol. 98, no. 4, pp. 384–390 (2023). <https://doi.org/10.6036/10879>
17. Gu, X., Velez, P.: On the dynamic simulation of eccentricity errors in planetary gears. *Mech. Mach. Theory* **61**, 14–29 (2013). <https://doi.org/10.1016/j.mechmachtheory.2012.10.003>
18. Vedmar, L., Henriksson, B.: A general approach for determining dynamic forces in spur gears. *J. Mech. Des.* **120**(4), 593 (1998). <https://doi.org/10.1016/j.jal.2010.01.013>
19. Fernandez del Rincon, A., Viadero, F., Iglesias, M., García, P., Sancibrian, R.: A model for the study of meshing stiffness in spur gear transmissions. *Mech. Mach. Theory* **61**, 30–58 (2013). <https://doi.org/10.1016/j.mechmachtheory.2012.10.008>
20. Sanchez-Espiga, J., Fernandez-del-Rincon, A., Iglesias, M., Viadero, F.: Numerical evaluation of the accuracy in the load sharing calculation using strain gauges: Sun and ring gear tooth root. *Mech. Mach. Theory* **175**, 104923 (2022). <https://doi.org/10.1016/J.MECHMACHTHEORY.2022.104923>
21. Weber, K., Banaschek, C.: *The Deformation of Loaded Gears and the Effect on their Load Carrying Capacity*. London (1951)
22. Zander, G., Kehl, M., Otto, J., Böttcher, M., Stahl, R., Poll, K.: Erweiterung LAGER2 – Erweiterung der Wälzlagerberechnung. In: *FVA-Software: Forschungsvorhaben*, vol. 701 III. F, no. 1404 (2020)

23. Jurkschat, T., Otto, M., Lohner, T., Stahl, K.: Determination of the loss behavior and thermal balance of rolling bearings. *Forsch. im Ingenieurwesen/Eng. Res.* **82**(2), 149–155 (2018). <https://doi.org/10.1007/s10010-018-0266-0>
24. Fernández-Del-Rincón, A., Iglesias, M., De-Juan, A., Diez-Ibarbia, A., García, P., Viadero, F.: Gear transmission dynamics: effects of index and run out errors. *Appl. Acoust.* **108**, 63–83 (2016). <https://doi.org/10.1016/j.apacoust.2015.11.012>